

## NUMERICAL AND EXPERIMENTAL ANALYSIS OF TUBE DRAWING WITH FIXED PLUG

### Frederico Ozanan Neves

Federal University of Sao Joao del Rei  
Praça Frei Orlando 170 – Centro  
36360-000 - São João del.- Rei –MG  
[fred@funrei.br](mailto:fred@funrei.br)

### Fernando César Gentile

State University of Campinas  
School of Mechanical Engineering  
Department of Materials Engineering  
C.P. 6122 - 13083-970 – Campinas – SP  
[gentile@fem.unicamp.br](mailto:gentile@fem.unicamp.br)

### Célio Caminaga

State University of Campinas  
School of Mechanical Engineering  
Department of Materials Engineering  
C.P. 6122 - 13083-970 – Campinas – SP  
[celioc@fem.unicamp.br](mailto:celioc@fem.unicamp.br)

### Sérgio Tonini Button

State University of Campinas  
School of Mechanical Engineering  
Department of Materials Engineering  
C.P. 6122 - 13083-970 – Campinas – SP  
[sergiol@fem.unicamp.br](mailto:sergiol@fem.unicamp.br)

**Abstract.** Numerical simulation of manufacturing processes has become in the last years an important tool to improve these processes reducing lead times and try out, and providing products free of defects and with controlled mechanical properties. Finite Element Method (FEM) is one of the most important methods to simulate metal forming. In tube drawing with fixed plug both the outer diameter and the inner diameter of the tube are properly defined if correct process conditions are chosen for the die angle, drawing speed, lubrication and area reduction per pass. These conditions have great influence on drawing loads and residual stresses present in the product. In this work, cold drawing of tubes with fixed plug was simulated by FEM with the commercial software MSC.Superform to find the best geometry of die and plug to reduce drawn force. An elasto-plastic model was used for the material of the tube, and the die and plug were considered elastic. A stainless A304 steel tube with initial dimensions of 10 x 1,5 mm (diameter x thickness) was drawn. The die and mandrel were modeled as being of tungsten carbide. The numerical analysis supplied results for the reactions of the die and plug and the stresses in the tube, the drawing force and the final dimensions of the product. Those results are compared with results obtained from analytic models, and also with experimental results from tests with a laboratory drawing bench. In these tests two lubricants with different viscosity were analyzed, and two dies were used to pressurize the lubricant and to establish a hydrodynamic lubrication.

**Keywords.** cold tube drawing, finite element analysis, profile die design, upper bound solution

### 1. Introduction

Superior quality products with precise dimensions, good surface finish and specified mechanical properties can be obtained with drawing processes. However, the design of optimized cold drawing by means of classical trials and errors procedures, based substantially on designers' experience, has become increasingly heavy in terms of time and cost.

In recent years, rapid development of computer techniques and the application of the theory of plasticity has made possible to use a more complex approach to problems of formability and plasticity of metals. Numerical simulation is a very useful tool to predict mechanical properties of the products and tools design optimization (Bethenoux et al., 1996). Pospiech (1997) presented a description of a mathematical model for the process of tube drawing with fixed mandrels. Karnezis and Farrugia (1966) had made an extensive study of tube drawing using finite element modelling.

In the present study, a series of experiments, numerical and analytical simulations were performed to analyze the material behavior as a function of the die and plug shape. The results were compared with experimental results obtained in tests with a laboratory drawn bench.

## 2. Plug geometry

Plug geometry is shown on Fig. 2. The region A is a cylindrical portion to position the plug inside the die. Its diameter is slightly smaller than the tube inner diameter. The plug semi-angle ( $\alpha_p$ ) is smaller than die semi-angle ( $\alpha$ ). It is suggested to be 2 degrees or more smaller than die semi-angle (Avitzur, 1983 and Pawelsky, O. and Armstroff, O., 1968).

Region C, called 'nib', is cylindrical and controls the inner diameter of the tube. In the present study the wall thickness of the tube was reduced of 0.1 mm. The length of the nib was fixed on 2 mm for all tests.

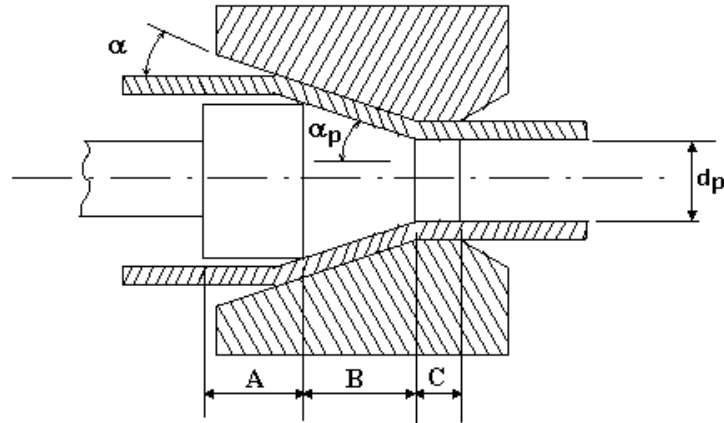


Figure 2 – Plug geometry.

Where:

$\alpha$  = die semi-angle

$\alpha_p$  = plug semi-angle

$d_p$  = nib diameter

## 3. Finite element model

Tube drawing process was simulated with the software MSC.Superform 2002 using a 3D finite element model as shown in Fig. 1. Tubes with dimension 10 x 1.5 mm (diameter x thickness) were drawn to three different area reduction, using four die angles for each reduction, as shown on Tab. 1. In all simulations, the wall thickness was reduced from 1.5 mm to 1.4 mm.

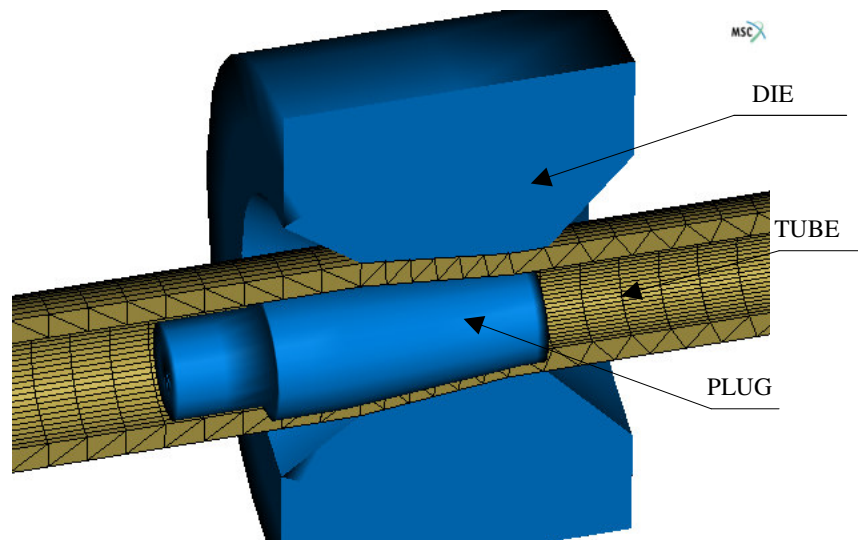


Figure 1 – FE meshes of tube, die and plug used in the numerical simulation

Table 1 – Area reductions and die angles used in the numerical simulation

Simulation #	Area reduction (%)	Die semi-angle (degrees)	Outlet diameter (mm)
1	34.4	7.0	7.94
2	34.4	8.8	7.94
3	34.4	10.0	7.94
4	34.4	14.0	7.94
5	26.5	7.0	8.40
6	26.5	8.8	8.40
7	26.5	10.0	8.40
8	26.5	14.0	8.40
9	20.0	7.0	8.76
10	20.0	8.8	8.76
11	20.0	10.0	8.76
12	20.0	14.0	8.76

A quarter piece of tube 100 mm long was modeled using a number of 3200 bricks elements with 8 nodes to define the mesh. This length was tested in order to obtain the steady-state condition. The die geometry consisted of a 30° half entry angle, a 15° half exit angle and bearing length of 0.4 times the outlet diameter.

Friction between die and tube and between tube and plug was estimated as 0.05, assumed to be Coulomb friction. Die and plug were modeled as an elastic material, assumed to be tungsten carbide (Young modulus of 700 GPa).

An elasto-plastic model was used for the material of the tube. Tensile tests of stainless A304 steel tube were hold to obtain the stress-strain curve ( $\sigma \times \epsilon$ ) applied to the simulation. This stress-strain curve was approached by Holloman's equation as shown in Eq. (1).

$$\sigma = 1137 \epsilon^{0.52} [\text{MPa}] \quad (1)$$

Young modulus of 210 GPa and a Poisson ratio of 0.3 were considered to tube material, which was assumed to be isotropic and insensitive to strain rate. During experimental drawing it was noticed that the temperature at the tube was not higher than 100 °C, thus allowing the tube material to be modelled as a material independent on the temperature.

#### 4. Analytical model

An upper bound solution (UBS) of tube drawing with fixed plug was obtained. The solution presented in this work is adapted from that obtained by Avitzur (1983) for tube sinking. This analytical model considered an isotropic strain-hardening material for the tube, a Coulomb friction, a cylindrical stress state, and the flow rule of Tresca. The process geometry is represented on Fig. 3. Equation (2) is the analytical expression of the tube drawing tension with fixed plug.

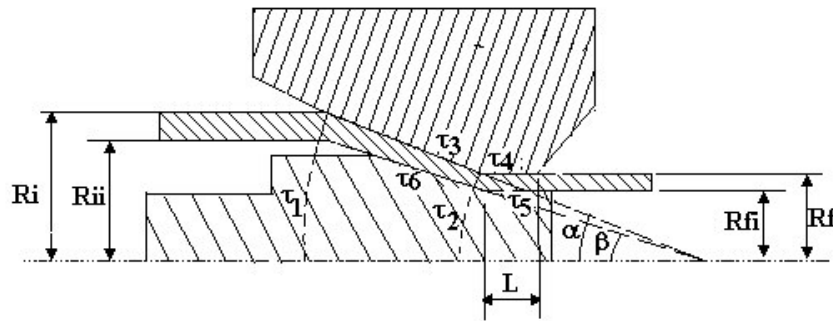


Figure 3 – Tube drawing with fixed plug

$$\sigma_{\text{tref}} = \sigma_0 \left\{ \frac{2f(\gamma) \ln \frac{R_i}{R_f} + \frac{2}{\sqrt{3}} \left[ \frac{\alpha}{\sin^2(\alpha)} - \cotg(\alpha) - \frac{\beta}{\sin^2(\beta)} + \cotg(\beta) \right] + B(1 - \ln \frac{R_i}{R_f}) \ln \frac{R_i}{R_f} + 2\mu_1 \frac{L}{R_f}}{1 + 2\mu_1 \frac{L}{R_f}} \right\} \quad (1)$$

where:

$$B = 2\{\mu_1 \cotg(\alpha) + \mu_2 \cotg(\beta)\} \quad (2)$$

and

$$f(\gamma) = \frac{1}{\text{sen}^2(\alpha)} \left[ \cos(\beta) \sqrt{1 - \frac{11}{12} \text{sen}^2(\beta)} - \cos(\alpha) \sqrt{1 - \frac{11}{12} \text{sen}^2(\alpha)} + \frac{1}{\sqrt{132}} \ln \left( \frac{\sqrt{\frac{11}{12} \cos(\beta)} + \sqrt{1 - \frac{11}{12} \text{sen}^2(\beta)}}{\sqrt{\frac{11}{12} \cos(\alpha)} + \sqrt{1 - \frac{11}{12} \text{sen}^2(\alpha)}} \right) \right] \quad (3)$$

$\sigma_0$  = average yield stress

$\alpha$  = die semi-angle

$\beta$  = semi-angle of the internal cone of the tube on drawing one

$\mu_1$  = Coulomb friction between the and die

$\mu_2$  = Coulomb friction between plug and tube

$\tau_1$  e  $\tau_2$  = Velocity subface discontinuity  $\tau_1$  e  $\tau_2$

$\tau_3, \tau_4, \tau_5$  e  $\tau_6$  = contact surfaces

$R_i$  = external inlet radius of the tube

$R_{ii}$  = internal inlet radius of the tube

$R_f$  = external outlet radius of the tube

$R_{fi}$  = internal outlet radius of the tube

$L$  = bearing length

## 5. Experimental tests

Stainless A304 steel tubes were drawn in a laboratory drawn bench. Tubes with 10 x 1.5 mm (diameter x thickness) were reduced to 7.94 x 1.4 mm, that represents a drawing pass with 34.4% of area reduction. Two dies were used, both made of tungsten carbide with die semi-angle of 7° and bearing length of 3 mm. One die has an exit diameter of 9.8 mm and the other an exit diameter of 7.94 mm.

The tube initial length was 500 mm. First, it was cold swaged to reduce one of its ends and to allow to pass it through the dies. Figure 4 shows an illustration of the die support. After the tube was located inside the die, the die support was filled with oil and closed to pressurize the chamber.

Tubes were drawn at a speed of 1.0 m/min and two lubricants were used: a common mineral oil SAE 20W50 (22 cSt at 100 °C), and MZA-20 (190 cSt at 100 °C), a mineral oil formulated with extreme pressure additives and grease, indicated to cold forming processes.

Plug was made of AISI D6 tool steel, quenched and tempered to 52 HC. Plug semi-angle was 5.4° with a nib length of 2 mm. Tube cavity was filled with the same oil used in die support, and then the plug was positioned at the work zone and fastened by a stick to the drawn bench structure.

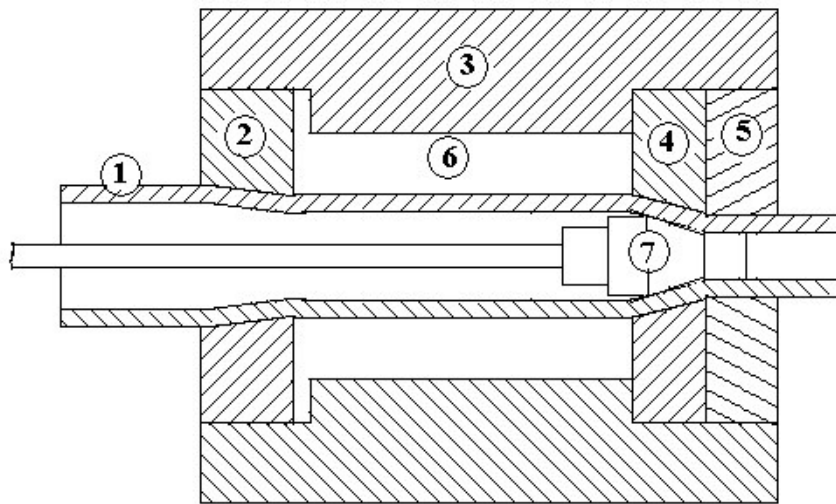


Figure 4 – Schematic representation of the die support, dies and tube.

In Figure 4:

- 1 – tube
- 2 – first reduction die
- 3 – die support
- 4 – second reduction die
- 5 – load cell
- 6 – pressure chamber
- 7 – fixed plug

## 6. Results

### 6.1. FEM analysis

Figure 5 shows the drawn stress (longitudinal stress) obtained from numerical simulation with the Finite Element Method previously discussed. It is seen that best die semi-angle is found between 7 to 10° for all area reductions simulated (20, 25 and 34,4%).

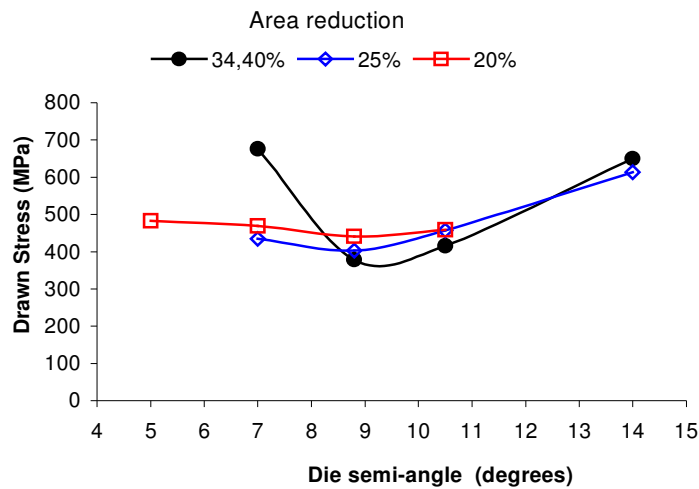


Figure 5 – Drawn stress x die semi-angle, predicted with FEM analysis.

Figure 6 shows the variation of equivalent stress for a point located at the outer surface of the tube, since the die entry until a point located 40 mm far from there, during the drawn pass with 34.4% of area reduction for each die semi-angle simulated. Note that the average equivalent stress is very unstable until beyond 10 mm and thereafter the process becomes stable.

In Fig. 7 it is shown the equivalent stress distribution along the tube with 34.4% of area reduction, die semi-angle of 7° and friction coefficient of 0.05 to plug-tube and die-tube interface. It can be seen that there is a great variation of equivalent stress through the die length and then next after the die exit the equivalent stress reaches an uniform value. The inner and outer exit tube diameter did not show any variation in all simulations.

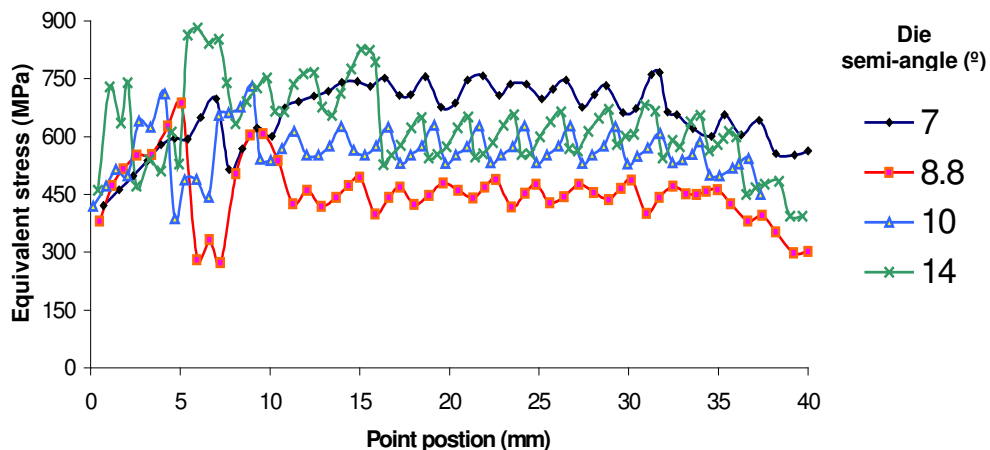


Figure 6 – Variation of equivalent stress of a point passing through the die.

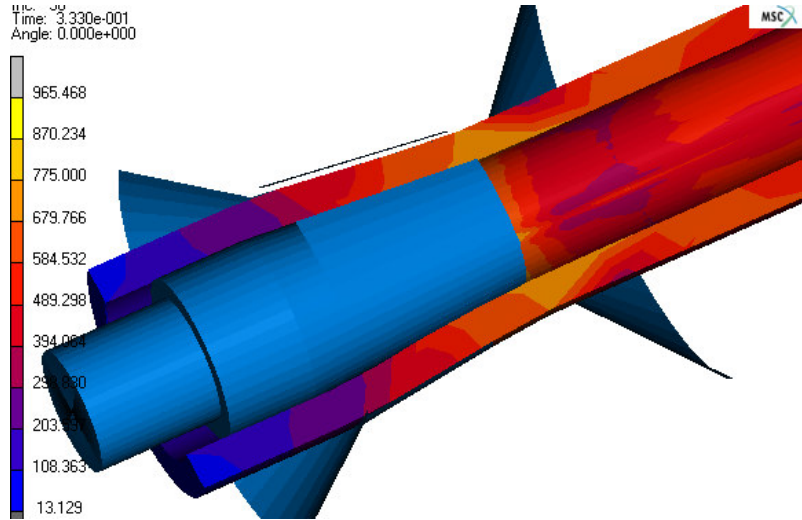


Figure 7 – Equivalent stress distribution along the tube.

## 6.2. Analytical results

Figure 8 shows the drawn stress variation with die semi-angle for the three area reduction studied where was assumed a Coulomb friction of 0.05 in all interfaces.

It can be seen that the results quite agree with drawn stress obtained from FE analysis. The best die semi-angles again were found between 7° and 10°, as FEM analysis had predicted.

Figure 9 shows the drawn stress for some values of friction coefficient adopted on die-tube interface and plug-tube interface. In curve 1 friction coefficient between die and plug was 0.05 and between tube and plug was 0.0, which represents a tube drawing without a plug. The friction coefficients used in curve 2 were 0.05 and 0.05, respectively. For curve 3, it was adopted 0.1 and 0.05, for curve 4, 0.1 and 0.1 and, finally, for curve 5, 0.05 and 0.1.

As it was expected, drawn stress increases with increasing friction on die-tube interface, as well as increasing friction on plug-tube interface. However, it can be noted that drawn stress increase more significantly with an increasing friction on plug-tube interface than on die-tube interface.

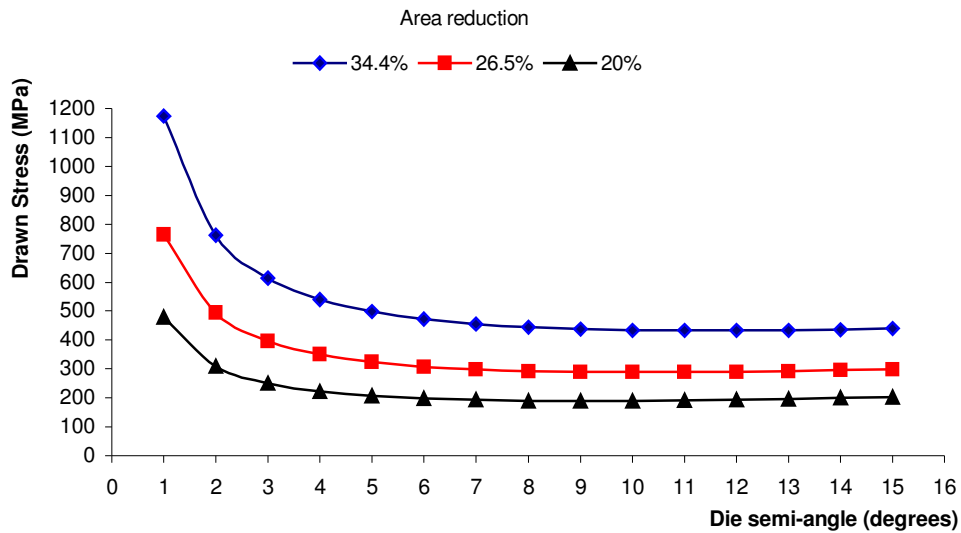


Figure 8 – Drawn stress variation with die semi-angle and area reduction, obtained with the upper bound method.

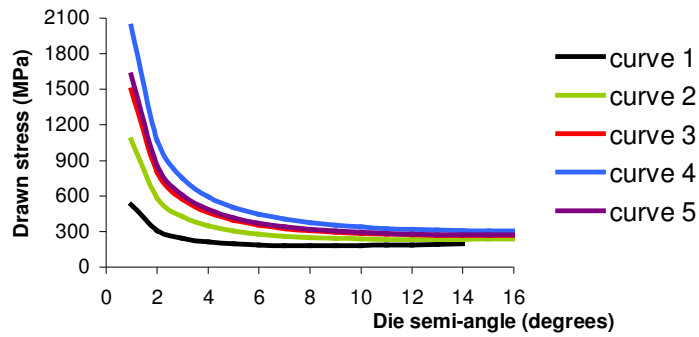


Figure 9 – Drawn stress calculated with upper bound method varying the die semi-angle and the friction coefficient on die-tube and plug-tube interfaces.

### 6.3. Experimental results

Results of experimental tests are shown in Fig. 10 and 11. There are shown three observations for tube drawn with fixed plug using SAE 20W50 mineral oil and MZA-20.

It can be observed in Figure 10 that in all tests that the process does not reaches a steady state while in Fig. 11 the process seems to reach it. Table 2 shows the mean drawn force for each observation, calculated from the moment the process begins till the moment it is finished. The drawn stress is calculated dividing the drawn force by the area of the drawn tube which is 34.9 mm<sup>2</sup>.

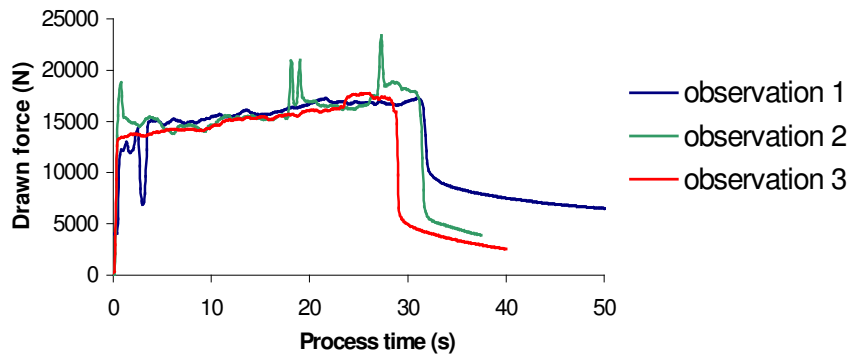


Figure 10 – Experimental tests results – Lubricant: SAE 20W50 mineral oil – drawn speed: 1.0 m/min

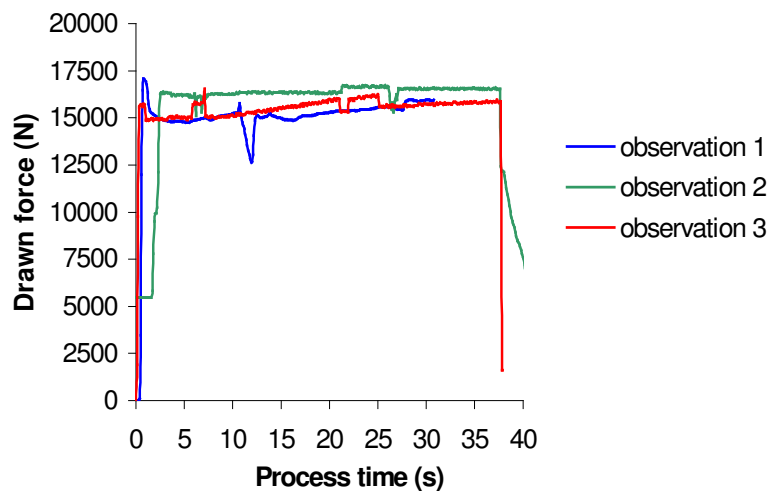


Figure 11 – Experimental tests results – Lubricant: MZA – 20 – drawn speed: 1.0 m/min

Table 2 – Mean drawn force and mean drawn stress - experimental results.

Observations	SAE 20W50		MZA – 20		FEM	UBS
	Mean drawn force (N)	Mean drawn stress (MPa)	Mean drawn force (N)	Mean drawn stress (MPa)	from Figure 7	from Figure 8
1	15716.21	450.32	15125.83	433.40	489	455
2	16084.02	460.86	16369.60	469.04		
3	16187.12	463.81	15599.20	446.97		
Mean value	15995.78	458.33	15698.21	449.81		

The mean values of the experimental results are in good agreement to that obtained in both FEM and analytical simulations with 34.4% of area reduction, die semi-angle of 7° and friction coefficient of 0.05 for both surfaces in contact with the tools.

A statistical analysis of the stress results (Montgomery, D. C., 1984), comparing treatments means from the two lubricants used in the tests, showed that there was no difference between them. The analysis of variance is shown on Tab. 3, and it be concluded that both lubricants show the same mean drawn stress since test value  $F_0$  is less than  $F_{0.05,1,2}$ .

Table 3 – Analysis of variance for the mean drawn stress.

Lubricant	Observation [MPa]			$\sum y.$	$\bar{y}$
	1	2	3		
SAE 20 W 50	450.32	460.86	463.8	1374.99	458.33
MZA 20	433.40	469.04	446.97	1349.42	449.81
				2724.41	454.07
SSt	856.75				
SStreat	108.03				
SSe	747.719				
$F_0$	0.22				
$F_{0.05,1,2}$	9.55				

## 7. Conclusions

1. FEM analysis is a powerful method to help process and tool designers;
2. The drawn loads measured in experimental tests with tools designed by FEM analysis are in good agreement with the numerical results;
3. The drawn load can be obtained with accuracy with the Upper Bound Solution analytical simulation. However, this method can not help to calculate the stress-strain distribution along workpiece;
4. Lubricants SAE 20W50 mineral oil and MZA – 20 showed the same lubrication performance when tubes were drawn at the speed of 1 m/min and showed similar mean drawn stress. However, with MZA-20 the process reached a steady-state flow, and therefore the drawn force required was lower for this lubricant.

## 8. Acknowledgement

Authors would like to thank FAPESP – Fundação de Amparo a Pesquisa do Estado de São Paulo for the financial support, MSC.Software Corporation for the software MSC.Superform 2002 and Fuchs do Brasil, that kindly gave us the lubricant MZA-20.

## 9. References

- Avitur, B. , 1983, “Handbook of metal-Forming Process”. John Wiley & Sons. N. York.
- Brethenoux G at all, 1996, “Cold forming processes: some examples of predictions and design optimization using numerical simulations”. J. of Mat. Proc. Tech., vol. 60 (1-4), pp. 555 – 562.
- Karnezis, P. E and Farrugia, D. C. J., “Study of cold tube drawing by finite-element modeling”, J. Mat. Proc. Tech. v. 80-81, 1998, p. 690-694.
- Montgomery, D. C., 1984, “Design and analysis of experiments”, John Wiley and Sons, N. York, 537 p.
- Pawelski, O. and Armstroff, O., “Untersuchen über das Ziehen von Stalrohren mit fligeden Dorn”, 1968, Stahl und Eisen, n. 24, 28, nov, pp. 1348 – 1354.
- Pospiech, J., 1998, “Description of a Mathematical Model of Deformability for the Process of Drawing Tubes on a Fixed mandrel”. J. of Mat. Eng. and Performance. v. 21, feb, p. 71- 78.